Cerebral Cortex July 2010;20:1630–1646
doi:10.1093/cercor/bhp227
Advance Access publication October 30, 2009

Color Selectivity of Neurons in the Posterior Inferior Temporal Cortex of the Macaque Monkey

Masaharu Yasuda[1,2,3], Taku Banno[1,2] and Hidehiko Komatsu[1,2]

[1]Division of Sensory and Cognitive Information, National Institute for Physiological Sciences, Myodaiji, Okazaki 444-8585, Japan and [2]Department of Physiological Sciences, The Graduate University for Advanced Studies (SOKENDAI), Myodaiji, Okazaki 444-8585, Japan

[3]Current address: Laboratory of Sensorimotor Research, National Eye Institute, NIH, Bethesda, MD 20892-2235, USA

We recorded the activities of neurons in the lateral surface of the posterior inferior temporal cortex (PIT) of 3 hemispheres of 3 monkeys performing a visual fixation task. We characterized the color and shape selectivities of each neuron, mapped its receptive field (RF), and studied the distributions of these response properties. Using a set of color stimuli that were systematically distributed in Commission Internationale de l'Eclairage-*xy* chromaticity diagram, we found numerous color-selective neurons distributed throughout the area examined. Neurons in the ventral region tended to have sharper color tuning than those in the dorsal region. We also found a crude retinotopic organization in the ventral region. Within the ventral region of PIT, neurons in the dorsal part had RFs that overlapped the foveal center; the eccentricity of RFs increased in the more ventral part, and neurons in the anterior and posterior parts had RFs that represented the lower and upper visual fields, respectively. In all 3 hemispheres, the region where sharply tuned color-selective neurons were concentrated was confined within this retinotopic map. These findings suggest that PIT is a heterogeneous area and that there is a circumscribed region within it that has crude retinotopic organization and is involved in the processing of color.

Keywords: color, inferior temporal cortex, primate, retinotopy, TEO, visual cortex

Introduction

Within the monkey visual cortex, color information is transmitted along the ventral visual pathway through areas V2 (Hubel and Livingstone 1987) and V4 (Zeki 1973; Schein and Desimone 1990) until it reaches the inferior temporal (IT) cortex (Tanaka et al. 1991; Komatsu et al. 1992). Lesion studies showing that damage to the IT cortex disrupts color discrimination (Horel 1994; Heywood et al. 1995; Buckley et al. 1997; Huxlin et al. 2000; Cowey et al. 2001) suggest the IT cortex plays an important role in the processing of color information in monkeys. But to fully understand how color information is processed, one must know how this information is distributed or localized within the IT cortex.

The IT cortex is divided into 2 parts (Iwai and Mishkin 1969): area TE, which includes the anterior and central IT cortex, and area TEO, which includes the posterior IT cortex (PIT) (Van Essen et al. 1990). In the present study, we will use the term PIT instead of TEO to avoid confusion, as TEO is also used more specifically to indicate a retinotopically organized area in the posterior IT cortex (see below). Neural recordings have shown that area TE contains a large number of color-selective neurons (Komatsu et al. 1992; Komatsu and Ideura 1993; Koida and Komatsu 2007; Matsumora et al. 2008). In addition, both positron-emission tomography (Takechi et al. 1997) and 2-deoxy-glucose (2-DG) imaging (Tootell et al. 2004) carried out during a color discrimination task have shown that color stimuli evoke strong activation within the PIT, suggesting that the PIT is involved in the processing of color information. Recent functional magnetic resonance imaging (fMRI) experiments have also shown activation by color stimuli in the PIT (Conway and Tsao 2006; Conway et al. 2007). In one of these studies (Conway et al. 2007), neural recordings were also conducted from the region within the superior temporal sulcus (STS). However, there has been no systematic investigation of the color selectivity of PIT neurons in the lateral surface of the IT gyrus where most previous studies of PIT have concentrated. In the present study, therefore, we systematically analyzed the color selectivity of individual PIT neurons using stimuli based on Commission Internationale de l'Eclairage (CIE)-*xy* chromaticity diagram and examined how color-selective neurons are distributed in the lateral surface of the IT gyrus of the PIT cortex. In addition, because it has been demonstrated that lesioning the PIT severely disrupts shape discrimination (Iwai and Mishkin 1969) and that many PIT neurons exhibit shape selectivity (Tanaka et al. 1991; Kobatake and Tanaka 1994; Brincat and Connor 2004), we also examined the shape selectivity of the same group of neurons using a set of geometrical shapes.

Finally, Boussaoud and colleagues conducted a detailed mapping of the receptive fields (RFs) in and around the PIT and demonstrated that there exists a crude retinotopy of the contralateral visual hemifield on the lateral surface of the IT cortex, between the anterior tip of the inferior occipital sulcus (IOS) and the anterior end of the posterior middle temporal sulcus (PMTS) (Boussaoud et al. 1991). These authors referred to this retinotopically organized area as the TEO. In the present study, we also conducted RF mapping and attempted to examine how such retinotopic organization is related to the neuronal color selectivity.

Materials and Methods

Behavioral Task

Three awake macaque monkeys (*Macaca fuscata*) were used for the experiments. All procedures for animal care and experimentation were in accordance with the National Institutes of Health Guide for the Care and Use of Laboratory Animals and were approved by the institutional animal experimentation committee.

During the experiment, monkeys were seated on a primate chair, facing a Cathode-ray tube (CRT) monitor at a distance of 56 cm. The monkeys were trained to fixate on a small white dot (fixation spot, 50 cd/m^2, 0.1°) presented at the center of the monitor. A trial started when the fixation spot turned on. When the monkeys maintained fixation for 500 ms, a visual stimulus was presented at a certain position on the monitor for 500 ms. If the monkeys maintained fixation for 760

ms after stimulus offset, the fixation spot disappeared, and a drop of sports drink was given as a reward. When the visual stimulus was presented at the foveal center, the fixation spot turned off for a period extending from 350 ms before visual stimulus onset until 260 ms after stimulus offset. The monkeys' gaze was monitored using a scleral search-coil technique (Robinson 1963). The monkeys were required to maintain fixation within an eye window (±1.5° for monkeys KM and LW and ±0.75° for monkey MA) throughout the trial. If the monkeys' gaze deviated from the eye window, the trial was aborted.

Surgery and Recording

Under general anesthesia, sterile surgery was conducted to attach a head holder and a recording chamber to the skull using dental cement and implanted bolts. The animal was first sedated by intramuscular injection of ketamine hydrochloride and then anesthetized with an intraveneous injection of sodium pentobarbital. The head holder was used to connect a monkey's head to the primate chair. A search coil was placed under the conjunctiva of 1 eye and was connected to a plug on top of the skull. The recording chamber was placed laterally on the skull to cover the PIT on the lateral surface of the IT gyrus, which we will simply refer to as PIT in the following text. After surgery, the monkey was allowed to recover for at least 1 week before the experiment began. During this period, antibiotic (Cefazolin sodium) was given every 12 h.

A hydraulic microdrive (Narishige) was used to penetrate the dura with varnish-coated tungsten microelectrodes (Frederick Haer) or elgiloy electrodes to record single and multiple neuron activities extracellularly. To precisely locate the electrodes, they were advanced through a stainless steel guidetube situated within a plastic grid in which holes were placed at intervals of 1 mm (Crist et al. 1988). By using 2 grids that were shifted 0.5 mm vertically and horizontally with respect to one another, a minimum interval of 0.7 mm between holes was attained.

Neuronal signals were amplified, sampled at 25 kHz, and stored on a computer for off-line analysis. Behavioral events were recorded at 1 kHz. To inspect the visual responses, neuronal signals were discriminated on the basis of spike amplitude, converted to pulses, and displayed online as rasters and peristimulus–time histograms (PSTHs). During each electrode penetration, we sampled neuron activities at every 100- to 300-μm interval, and tested the color–shape selectivities. Neuronal signals and discriminated pulses also were fed to a speaker for audio monitoring. After several electrode penetrations, markings were made by passing tiny currents through the tip of the electrode.

At the end of the experiments, the monkeys were deeply anesthetized with sodium pentobarbital and perfused via the heart, first with saline and then with 4% paraformaldehyde plus 2% ferrocyanide. The brain was then removed from the skull, sectioned in the frontal plane, and stained with cresyl violet. The sites of electrode markings were identified on the histological sections under microscopic examination.

Determination of the Recording Sites

An important problem in this study was how to define the extent of the PIT, which cannot be clearly segregated, cytoarchitectonically (Bonin and Bailey 1947) or mieloarchitectonically (Boussaoud et al. 1991), from the surrounding regions (e.g., areas TE and V4). Lesion studies have commonly employed sulcal landmarks to delineate the boundary of the PIT (Heywood et al. 1995; De Weerd et al. 1999; Huxlin et al. 2000; Cowey et al. 2001); its posterior border is at or just anterior to the anterior tip of the IOS, and the anterior border is at the anterior end of the PMTS. In the present study, we determined the extent of the recording sites based on the same sulcal landmarks. Before surgery, the position of the STS, the IOS, and the PMTS were identified on MRI scans. The recording chamber was placed so as to cover the region anterior to the IOS and the region around the PMTS, but the exact position and orientation differed across hemispheres, as described in Results. For 2 hemispheres (monkeys KM and LW), electrode penetrations were made roughly perpendicular to the cortical surface, and the penetration sites were mapped based on the coordinates of the grid used to guide the electrode. For the remaining hemisphere (monkey MA), electrode penetrations were made obliquely to the IT gyrus, and we confirmed the location of the electrode by taking X-rays (Toshiba TR-80A-ES-L, 70 kV, 20 mA, and 0.4 s) at the end of most recording sessions. For this hemisphere, we then constructed a 2D unfolded map of the recorded sites (see Results) based on the X-ray pictures of the electrode and MRI images of the brain. The gray matter could be clearly seen in the MRI image, and we used the midline of the gray matter to construct the unfolded map of the cortex (Van Essen and Maunsell 1980). We identified the recording site of each neuron on the MRI image based on the depth profile of the electrode track and by superimposing the X-ray image of the electrode on the MRI image (Fig. 2*C*). The results were plotted on the unfolded map by projecting each recording site onto the midline of the gray matter.

Visual Stimuli and Test of Selectivity

Visual stimuli were generated using a graphics board (VSG2/3, Cambridge Research) in a computer and displayed on a CRT monitor (Sony GDM-F500R; 800 × 600 pixels, 40° horizontally × 30° vertically; 142 frames/s). Figure 1 shows the standard set of colors and shapes used. Stimulus colors were defined on the basis of the CIE 1931 *xy* chromaticity diagram (Fig. 1*A*). The shaded triangular region indicates the range of colors that could be displayed by the CRT monitor used. We used 2 sets of color stimuli to test the color selectivity of neurons. Each set consisted of 15 colors whose chromaticity coordinates were evenly distributed on the chromaticity diagram (1–15 in Fig. 1*A*). In one set (bright color set), all stimuli had the same luminance (20 cd/m^2), except for the blue color (#15, 12 cd/m^2), and all were brighter than the gray background (10 cd/m^2, $x = 0.3127$, $y = 0.3290$,). Because the luminance for blue (#15 color) was different from the other colors, we omitted the responses to this color from the analysis. In another set (dark color set), the luminance of all 15 stimuli was the same (5 cd/m^2) and darker than the background. In addition to the 15 colors, a neutral gray stimulus ($x = 0.3127$, $y = 0.3290$) with the same luminance (either 20 or 5 cd/m^2) was also tested (W in Fig. 1*A*). To coarsely test for color selectivity, we used another set of 16 colors that consisted of 7 colors (1, 3, 5, 10, 12, and 15 and W in Fig. 1*A*) at 2 luminance levels (5 and 20 or 12 cd/m^2 for bright blue) together with white and black stimuli. This stimulus set was used only for qualitative examination of the color selectivity. When we tested color selectivity, the shape of the stimuli was fixed and chosen from 11 geometrical shapes (Fig. 1*B*; square, diamond, circle, star, cross, oblique cross, triangle, vertical bar, and oblique bar in the clockwise direction, horizontal bar and oblique bar in the counterclockwise direction). Each of these shape stimuli was painted homogeneously with a single color. To test the shape selectivity of neurons, we usually used these 11 shapes, but in some experiments, the 4-bar stimuli were not tested. The chromaticity coordinates and the luminance of the stimuli were measured using a spectrophotometer (PhotoResearch PR-650).

For each single neuron or multiple neurons, we determined the optimum stimulus color, shape, position, and size. Stationary flash stimuli were used in all the experiments. To test the color (shape) selectivity, the shape (color) of the stimuli was fixed to the optimum parameters for the neuron under study. We explored the optimum parameters for each neuron as follows: We first tested color selectivity using a certain shape (usually circle or the optimal shape for the neuron tested immediately before). If some response was obtained, we tested shape selectivity using a color that evoked the strongest response. Then, we retested the color selectivity using the shape that evoked the strongest response. We repeated such a cycle until we found the optimal combination of the color and shape. If no response was obtained at the initial test of color selectivity, we tested shape selectivity using 3 different colors (colors #7, 8, and 11 in Fig. 1*A*). If some response was obtained during this screening of an appropriate shape, we started the examination of color selectivity using that shape. If we failed to drive the neuron by these procedures, we advanced the electrode to examine another neuron. A neuron was regarded as visually responsive if it showed higher activity during the presentation of one or more of the stimuli used in the experiment. The stimulus size used for visually responsive neurons was on average 1.86° (25% quartile: 1.12°, 75% quartile: 2.24°) that was defined as the square root of the area of the stimulus and was in general much smaller than the RF.

Color and/or shape selectivity was first examined qualitatively by inspecting the online PSTHs and audio monitoring the responses. Responses were judged to be selective if there was a clear difference in

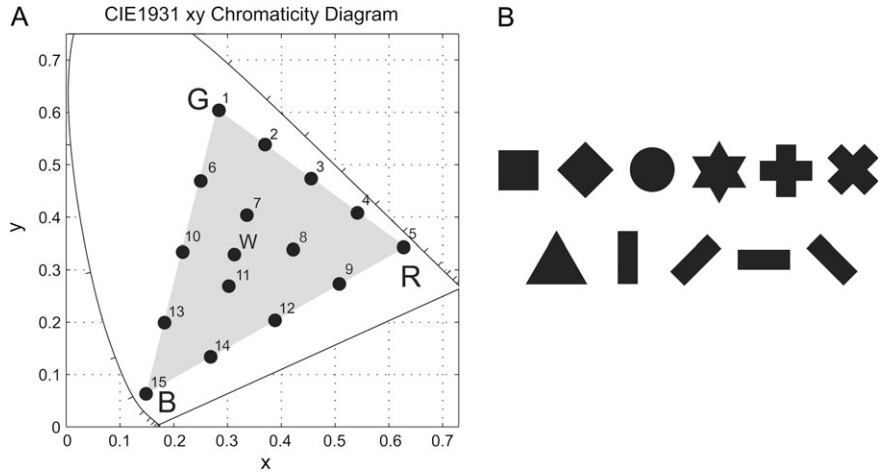

Figure 1. *A*) Standard set of colors used to test color selectivity. The chromaticity coordinates of each color are indicated by a spot on the CIE 1931 chromaticity diagrams. R, G, and B indicate the positions of the 3 primary colors of the monitor we used in the experiments. Test colors included 15 colors that evenly covered the portion of the CIE-*xy* chromaticity diagram delimited by the 3 primary colors. In some experiments, we also used a neutral gray (W). (*B*) Standard set of 11 geometric shapes used to test shape selectivity: square, diamond, circle, star, cross, oblique cross, triangle, vertical bar, oblique bar in the clockwise direction, horizontal bar and oblique bar in the counterclockwise direction. During testing, each shape stimulus was painted homogeneously with the same color.

the response magnitudes across stimuli. In about one-third of the visually responsive neurons, neural signals were recorded for off-line analysis, and stimulus selectivity was examined quantitatively. We did not attempt to record all visually responsive neurons for off-line analysis because the priority was to sample the neurons at regular intervals throughout the entire course of the penetration and test the stimulus selectivities to complete the functional mapping. Sampling of neurons for the off-line analysis did not involve any selection criteria other than the responsiveness to visual stimuli. During the recordings for off-line analysis, a stimulus was chosen randomly from the stimulus set in each trial, and trials were repeated until each stimulus was presented at least 6 times.

Data Analysis

Off-line quantitative data analysis was conducted only for single neurons. For off-line analysis of neuronal data, we first used a template-matching algorithm with temporal resolution of 1 ms to isolate spikes. We then computed the average firing rate of the isolated spikes during the stimulus presentation period (50–550 ms after stimulus onset), taking into account a response latency of about 50 ms. From this average, we subtracted the firing rate before stimulus presentation (300–0 ms before stimulus onset, baseline activity), and the resultant rate was taken as a measure of the neuronal response to the visual stimulus. Only neurons whose responses to the optimal color were larger than 10 spike/s and whose discharge rates during presentation of the optimal color were significantly different from baseline (Student's *t*-test, $P < 0.05$) were included in the sample for analysis. A small number of neurons (2 neurons for monkey KM, 2 for LW, and 1 for MA) did not meet this criterion and were excluded from the quantitative analysis.

To quantify the strength of the color selectivity of each neuron, a selectivity index was calculated as 1 − (minimum response)/(maximum response). We also used one-way analysis of variance (ANOVA) to evaluate whether the variation in the responses to stimuli within a set of test stimuli was significant. When the selectivity index was larger than 0.6 (i.e., the maximum response was more than 2.5 times the minimum response) and response variation was significant (ANOVA, $P < 0.05$), the neuronal responses were regarded as stimulus selective. To quantify the sharpness of the stimulus selectivity, we calculated a sparseness index (Rolls and Tovee 1995; Vinje and Gallant 2000), which was defined as

$$\text{sparseness index} = \left[1 - \left(\sum_{i=1,n} r_i/n\right)^2 \Big/ \sum_{i=1,n} \left(r_i^2/n\right)\right] \Big/ (1 - 1/n),$$

where r_i is the firing rate to the ith stimulus in the set of n stimuli. If r_i was a negative value, it was replaced to zero. This index indicates the degree to which responses are unevenly distributed across the set of stimuli. We used this modified version of the sparseness index (Vinje and Gallant 2000) because it should be more intuitive if sharper selectivity yields a larger value of the index. When all stimuli evoke the same response amplitude, the sparseness index is minimum and has a value of 0. As the stimulus selectivity sharpens, the index becomes larger. If only one stimulus among the set evokes a response, the index value is at a maximum and is equal to 1. When we tested the color selectivity at 2 luminance levels, we determined these indices of color selectivity based on the responses obtained at the luminance that elicited the largest response.

We mapped the RFs for each neuron online by presenting the preferred stimulus at various positions on the CRT display and determining the horizontal and vertical extents of the RF. After identifying the optimal position, we examined the extent of the RF by shifting the position of the stimulus along the horizontal and vertical lines passing through the optimal position. Along these lines, we determined the border of the RF as the midpoint between the last position where we could obtain a clear response and the first position where we could not get any clear response. The horizontal and vertical extents of the RF was determined as the intervals between the borders identified in the way as described above. To investigate the distribution of RFs across the recorded area, we classified neurons according to the position of the RF center that was defined as the midpoint of the vertical and horizontal extents of the RF. RFs with eccentricities of less than 2.5° from the foveal center were classified as being in the "fovea." For the remaining neurons, we classified the RF into 3 groups depending on the position of its center. If the RF center was located within upper (lower) visual field and was located within ±60° of the polar angle from the vertical meridian, the RF was classified as being in the "upper (lower) visual field." In other cases, the RF was classified as being on the "horizontal meridian." When the entire RF border was not determined, we classified the RF into the same 4 groups according to the mean position of the RF extent that could be determined.

Results

Recording Sites within the PIT

We recorded neuronal activities in 3 hemispheres of 3 monkeys (monkeys KM, LW, and MA). This included a total of 953 single and multiple PIT neurons (KM: 289, LW: 418, and MA: 246). We also recorded neuronal activities in area V4 and in the superior temporal gyrus (see Figs. 3, 10, and 12), but

these neurons were excluded from the analysis in this paper. Of the 953 PIT neurons, 588 showed visual responses (KM: 225, LW: 220, and MA: 143) (Tables 1–3). We examined the color and shape selectivity of these neurons, mapped their RFs, and determined the spatial distribution of their response properties. We found that many neurons sharply tuned for color were situated in the region around the PMTS and that this region had a crude retinotopy. Figure 2*B* shows MRI images of the recorded hemispheres. As can be seen, the PMTS was located more ventrally in monkey MA than in monkeys KM and LW. Consequently, it was easier to access the cortex near the PMTS in monkeys KM and LW than in monkey MA, and we were able to conduct more extensive mapping of this region in these 2 monkeys. In the following, we will first present the results obtained from monkey KM in detail and then describe the results obtained from monkeys LW and MA.

Distribution of Color–Shape Selectivity in the PIT of Monkey KM

Figure 3*A* shows the sites at which neurons were recorded in the brain of KM; the red square indicates the position of the recording chamber. The recorded sites covered the region both dorsal and ventral to the PMTS. Because the rostral edge of the IOS was located at the posterior end of the chamber, we believe that most of the recorded sites were within the PIT (see Fig. 2*A*). Figure 3*B* shows an example of a marking at the tip of an elgiloy electrode; the penetration site of this electrode is indicated by arrows in Figure 3*A* and *C*. We found that a large number of neurons responded differently to certain colors in the stimulus set (color-selective neurons). These color-selective neurons were widely distributed across the recorded sites. Table 1 indicates the sample of neurons examined in KM. Of the 225 visually responsive neurons recorded, we tested color selectivity and/or shape selectivity in 195 neurons. Of these 195 neurons, we determined both the color and shape selectivities in 143 neurons (67 neurons quantitatively examined + 76 neurons qualitatively examined). The distribution of stimulus selectivity among these neurons is shown in Figure 3*C*, where the stimulus selectivity of each neuron is indicated by a symbol plotted at the grid coordinates of the penetration site. Red symbols represent color-selective neurons, and it can be clearly seen that most of the neurons were color selective (130/143: 90.9%). Some of these neurons (86/130: 66.2%) also showed shape selectivity (red stars), whereas others (44/130: 33.8%) did not (red circles), and the spatial distributions of these 2 types of neurons overlapped.

Table 1
Sample of neurons from monkey KM

Total recorded: 289	
Visually responsive: 225	
Color	Quantitatively examined 78
	Qualitatively examined 104
Shape	Quantitatively examined 81
	Qualitatively examined 75
Both color and shape	Quantitatively examined 67
	Qualitatively examined 76
Visually nonresponsive: 64	

Table 2
Sample of neurons from monkey LW

Total recorded: 418	
Visually responsive: 220	
Color	Quantitatively examined 70
	Qualitatively examined 118
Shape	Quantitatively examined 56
	Qualitatively examined 132
Both color and shape	Quantitatively examined 53
	Qualitatively examined 104
Visually nonresponsive: 198	

Table 3
Sample of neurons from monkey MA

Total recorded: 246	
Visually responsive: 143	
Color	Quantitatively examined 21
	Qualitatively examined 84
Shape	Quantitatively examined 18
	Qualitatively examined 98
Both color and shape	Quantitatively examined 18
	Qualitatively examined 73
Visually nonresponsive: 103	

Color-Selective Responses within the PIT

Figure 4 shows the responses of 3 representative color-selective single neurons recorded in the PIT of monkey KM. The responses to the standard sets of color and shape stimuli are shown by rasters and histograms on the left side. To the right, in the top panels, response magnitudes to color stimuli are represented by the diameters of circles and are plotted at positions that correspond to their chromaticity coordinates. In the bottom panels, responses to shape stimuli are plotted as line graphs. In all 3 neurons, clear differences in response magnitude were observed with different colors. The color-selectivity indices for these neurons were all larger than 0.6 (1.09, 1.0, and 1.47 for *A*–*C*, respectively), and they all showed statistically significant response variation across colors (ANOVA, $P < 0.05$). The neuron whose responses are illustrated in Figure 4*A* strongly responded to red colors, and that in Figure 4*B* responded selectively to blue and cyan colors. The neuron in Figure 4*C* showed both on and off responses; it showed a selective on response when green colors were presented and a selective off response when purple colors were turned off. Interestingly, the color evoking the on response and that evoking the off response are complementary to one another. We observed this combination of on and off responses to complementary colors in 4 PIT neurons: The combination of the colors for on- and off responses were yellow/blue, yellow–green/purple, yellow/purple, and cyan/red. The neurons in Figure 4*A* and *C* did not exhibit shape selectivity (selectivity index = 0.42 and 0.32 in *A* and *C*, respectively), whereas the neuron in Figure 4*B* showed clear shape selectivity, responding most strongly to the oblique cross shape (selectivity index = 1.01).

The preferred color and the strength and sharpness of the color selectivity differed from cell to cell. Figure 5 shows the responses of 8 representative color-selective neurons. Of these, 6 (from *A* to *F*) had sharp color tuning, and responses were evoked only by a specific range of hues; the preferred hues were cyan (*A*), blue (*B*), green (*C*), yellow (*D*), red–purple (*E*), and achromatic colors around gray (*F*), respectively. As a group, these sharply tuned color-sensitive neurons appear to represent the entire color space examined. Another neuron (*G*) showed broader color tuning that covered wide regions of the

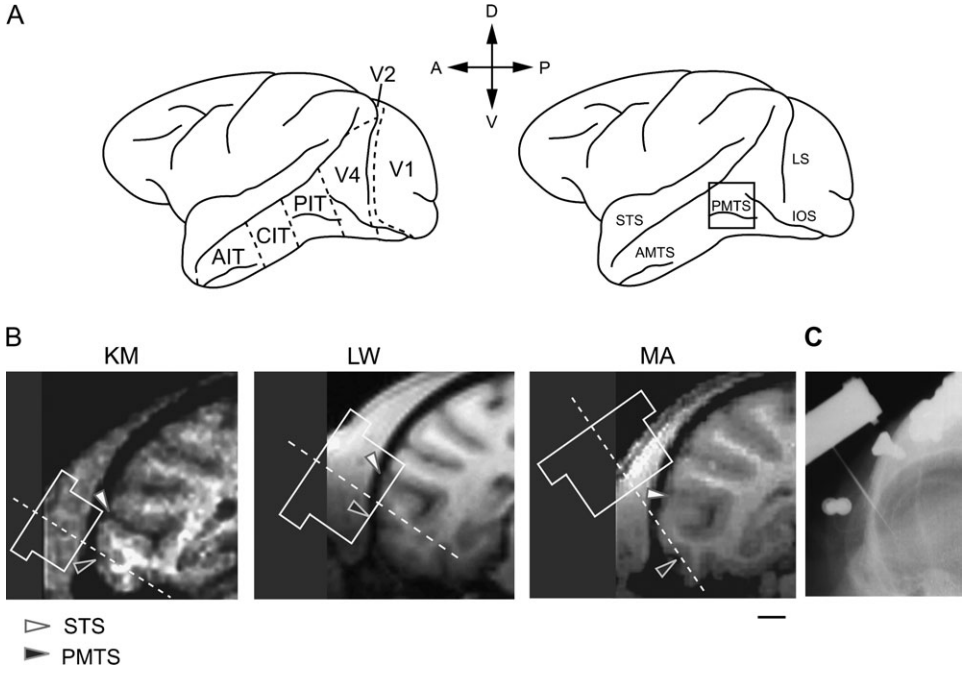

Figure 2. (*A*) Lateral view of the left hemisphere of monkey KM. The areas involved in the ventral stream are indicated. The IT cortex is divided into 3 parts: the AIT, anterior IT; CIT, central IT; and PIT, posterior IT. The PIT extends from the rostral edge of the IOS to the rostral edge of the PMTS in an anteroposterior direction. The black square indicates the area covered by the recording chamber used for monkey KM. (*B*) MRI images showing coronal sections including the PIT of the left hemispheres of 3 monkeys KM, LW, and MA in which the neural recordings were made. The stereotaxic coordinate is anterior 3 mm for KM, 5 mm for LW, and 6 mm for MA. The scale bar is 5 mm. The position and size of the recording chambers used are indicated by white contours, and the broken line indicates the direction of electrode penetration. The size of the recording chamber was larger for monkeys LW and MA than KM. The positions of the STS and PMTS in each hemisphere are indicated by white and black arrowheads, respectively. In monkey MA, the PMTS is more ventrally situated than in other monkeys. (*C*) X-ray image of MA with an electrode penetrated in the brain. The electrode can be clearly visible to the tip as a thin white line. AMTS, anterior middle temporal sulcus; IOS, inferior occipital sulcus; LS, lunate sulcus; PMTS, posterior middle temporal sulcus; STS, superior temporal sulcus; A, anterior; D, dorsal; P, posterior; and V, ventral.

chromaticity diagram, and the remaining neuron (*H*) had only marginal color selectivity (selectivity index = 0.63).

Concentration of Sharply Tuned Color-Selective Neurons in the PIT

We found that sharply tuned color-sensitive neurons, like those shown in Figure 5*A–F*, tended to be concentrated in the posteroventral two-thirds of our recording sites. This can be seen from the distribution of the sparseness indices, which indicate the sharpness of the color tuning (Fig. 6). In this figure, the sparseness index of single neurons in which color selectivity was quantitatively examined is shown at the grid coordinates where each neuron was recorded. The neurons shown in Figure 5 had sparseness indices of 0.82, 0.62, 0.48, 0.42, 0.42, 0.34, 0.25, and 0.03, from *A* to *H*, respectively, and are labeled accordingly. All 6 neurons that showed sharp color tuning (*A–F*) had sparseness indices of larger than 0.3, whereas the 2 neurons with broad color tuning (*G,H*) had sparseness indices less than 0.3. It can be seen in Figure 6 that many neurons in the posteroventral two-thirds of the recorded sites below the dotted line (light gray region) had indices larger than 0.3 (red font), whereas only a small number of neurons in the remaining more dorsal area above the dotted line (dark gray region) did. This tendency did not change, even when different sparseness indices (e.g., 0.4) were used as the cutoff criterion. Thus, although color-selective neurons are widely distributed within the PIT, the region is apparently not homogeneous with respect to the sharpness of the color selectivity of the neurons and should be divided into at least 2 subregions (dorsal and ventral). The fact that neurons with sharp color tuning are mainly situated in the ventral subregion across the PMTS suggests this area is more strongly related to the processing of color information than the more dorsal part of the PIT examined. In the following, therefore, we will distinguish the dorsal and the ventral subregions and tentatively refer to the latter as the PIT color area (PITC). Although determining the border is an important problem, we need much more dense mapping to precisely locate the border. In the present study, we have drawn the border of the PITC by connecting the recording sites where the proportion of cells with a sparseness index larger than 0.3 was equal to or more than 0.5.

Quantitative Analysis of Color and Shape Selectivities of PIT Neurons

To systematically examine the color and shape selectivities of neurons in the 2 subregions of the PIT, we calculated the selectivity and sparseness indices of each neuron; the distributions of these indices are shown for the neurons within the PITC (*Fig. 7A,B,E,F*) and for those recorded outside the PITC (*Fig. 7C,D,G,H*). Filled bars indicate neurons that were classified as color-selective (*A–D*) or shape selective (*E–H*). With respect to color selectivity, most PITC neurons (44/55, 80%) had selectivity indices greater than 1, and also the same proportion of cells (44/55, 80%) had sparseness indices larger than 0.3, which means that many PITC neurons are strongly and sharply color selective. On the other hand, neurons recorded outside the PITC tended to have smaller selectivity indices than those situated inside the PITC, and most had sparseness indices

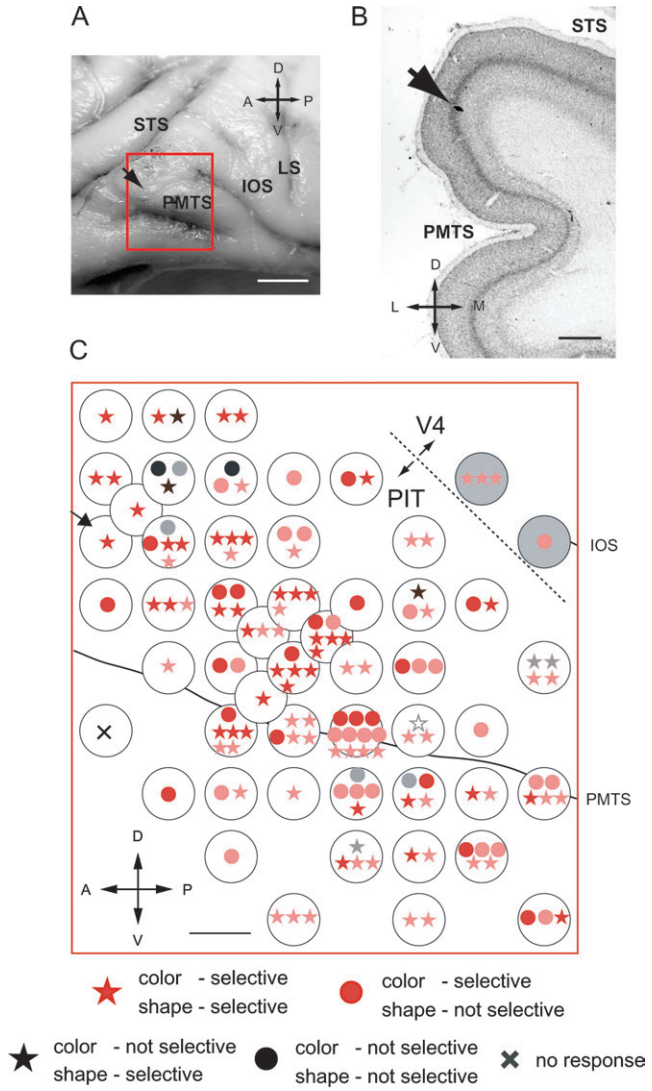

Figure 3. Recording sites in the brain of monkey KM and the distribution of color–shape selectivities. (*A*) Enlarged view of the recording sites shown on the brain of monkey KM. A red square indicates the area covered by the recording chamber. To confirm the position of the recording chamber, in some tracks, we made markings at the electrode tip by electrolytic deposition of iron from an elgiloy microelectrode. An arrow indicates a penetrated site where one of these markings was placed. (*B*) Coronal section of the PIT of monkey KM stained with cresyl violet. This section contained one of the markings, which is indicated by an arrow. This is the same marking shown in (*A*). (*C*) Stimulus selectivity of neurons across the surface of the PIT cortex. The stimulus selectivity of each neuron is indicated by a symbol plotted at the grid coordinates of the electrode penetration site. White circles indicate the holes in the grid used for electrode penetrations. Red symbols indicate color-selective neurons; black symbols indicate neurons that are not color selective. Stars indicate shape-selective neurons; circles indicate neurons that are not shape selective. Open stars indicate neurons that preferentially responded to either a black or white stimulus. Bold and pale symbols indicate that the stimulus selectivity was determined quantitatively and qualitatively, respectively. A cross indicates that neurons recorded from this site were not driven by the visual stimuli used. The arrow near the left-top corner indicates the site where the electrode marking shown in (*A*,*B*) was made. A dashed line near the right-top corner indicates the presumed border between the PIT and area V4. The 2 recording positions at the top right corner are located within the IOS and were excluded from our analysis. L, lateral; M, medial. Other abbreviations are the same as in Figure 2. Scale bar, 5 mm in (*A*), 1 mm in (*B*,*C*).

smaller than 0.3 (18/23, 78.3%). As expected, the proportion of the neurons inside the PITC that were sharply tuned for color (sparseness index > 0.3) was significantly larger than the proportion in the region outside the PITC (chi-squared test, $P < 0.05$), that is, neurons located outside the PITC had a weaker and broader color selectivity than PITC neurons.

With respect to shape selectivity, we found no clear difference between neurons located inside and outside the PITC. Shape selectivity indices were widely distributed from large to small both inside and outside the PITC (Fig. 7*E*, selective: $n = 31$, nonselective: $n = 18$, Fig. 7*G*, selective: $n = 22$, and nonselective: $n = 10$). The distributions of sparseness indices in both areas were biased toward small values, indicating that neurons in both subregions tended to have broad tuning to the shapes used in the present study.

Retinotopic Organization of the PIT

It was previously reported that the lateral surface of the PIT has a crude retinotopic organization (Boussaoud et al. 1991; Hikosaka 1998). To determine whether the region in which we recorded was similarly organized, we mapped the RFs of a large number of neurons and examined how they were distributed across the recorded area. In Figure 8*A*, the RFs of the recorded neurons are overlaid within the circles plotted at the grid coordinates of the electrode penetrations. The center of each circle indicates the foveal center, and the edge corresponds to 20° of eccentricity. When the RF extended outside the circle, the border of the RF was shaded to indicate which part was inside of the RF. The number of grid positions plotted in Figure 8 is different from that in Figure 6 because we could not map the RFs of all the neurons that were tested for color selectivity and vice versa. A small number of neurons did not respond to a stimulus presented at the fovea, although their RF overlapped the foveal center (the RF border drawn by a dotted line). In these neurons, the locations where the stimulus evoked the response continuously enclosed the foveal center although no response was evoked when the stimulus was presented at the foveal center.

The positions and extents of the RFs varied depending on the recording site. In the dorsal half of the recorded region, most neurons had relatively small RFs enclosing the foveal center. In the ventral half, the RFs were larger, and their centers were shifted out of the fovea, so that these neurons represented more peripheral visual fields. We also found that neurons in the anterior part of the ventral half had RFs mainly representing the lower visual field, and those in the more posterior part had RFs mainly representing the upper visual field, which suggests there is retinotopic organization in this region. To confirm that idea, we classified the RFs into 4 categories, based on their position and extent, and examined how each RF category was distributed among our recording sites. The 4 categories were "fovea," "upper visual field," "lower visual field," and horizontal meridian (see Materials and Methods). We adopted this categorical procedure because it appeared that, even if it existed, the retinotopy in this area was rather crude. In Figure 8*B*, the category of each RF is indicated by a symbol and plotted at the grid coordinates of electrode penetration. In the dorsal half of the PITC, most RFs overlapped the foveal center. In the ventral half, the RFs shifted to more peripheral visual fields, and neurons with RFs in the lower visual field and those with RFs in the upper visual field were clearly segregated in the anterior and posterior parts, respectively. Outside of the PITC, however, many neurons had RFs containing the foveal center but no systematic variation in the position of the RFs was observed. Overall, the crude retinotopy we observed in the PITC is consistent with the

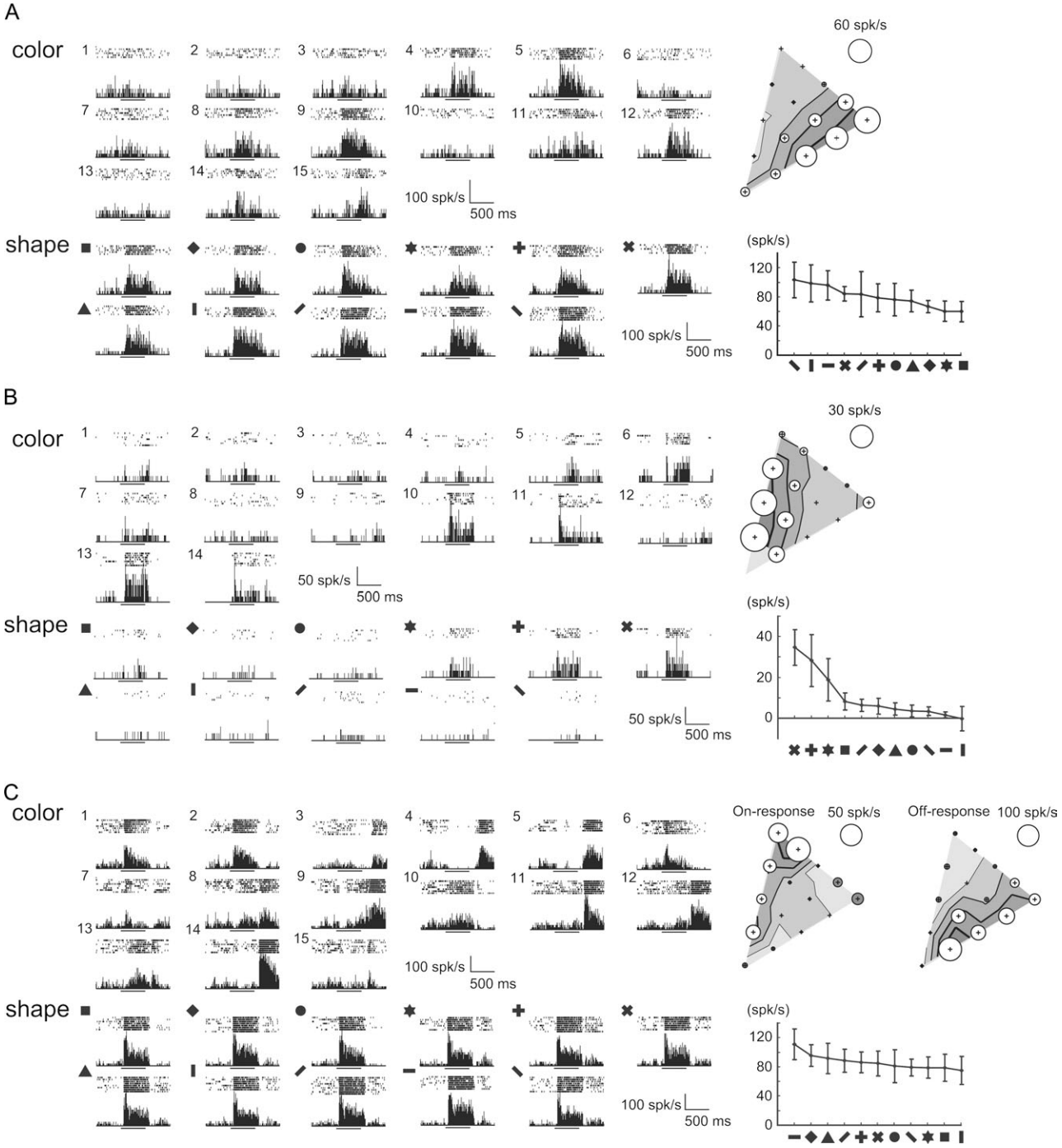

Figure 4. Color and shape selectivity of 3 example PIT neurons are shown in (*A–C*), respectively. Histograms and rasters show the responses of the neurons to 15 colors and 11 shapes. Each stimulus was presented for a 500-ms period indicated by the thick horizontal line below each histogram. Responses to color stimuli are shown on the top row, and those to shape stimuli are shown on the bottom row. The number of the presented color and the shape of the geometric stimulus are shown at the top left of each histogram. The color number corresponds to that shown in Figure 1*A*. To the right, in the top panels, response magnitudes to color stimuli are represented by the diameters of circles plotted at positions that correspond to their chromaticity coordinates. Open and solid circles indicate excitation and suppression, respectively. Contour lines indicate 75%, 50%, 25%, and 0% of the maximum response. In the bottom panels, responses to shape stimuli (mean ± standard deviation) are plotted as a line graph. dark color set was used to test color selectivity for the neurons in (*A*,*C*). A bright color set was used for that in (*B*). When the bright color set was used, responses to color #15 (blue) was omitted from the analysis because this color had a different luminance from the other colors (see Materials and Methods for detail).

retinotopic organization of the TEO described by Boussaoud et al. (1991).

Recordings from the PIT of Monkey LW

Figure 9*A* shows the sites at which neurons were recorded in the brain of LW; the square indicates the position of the recording chamber. Most of the recordings were made from the region anterior to the IOS that corresponds to the PIT, but some recordings were made from the region posterior to the IOS corresponding to V4. Like monkey KM, the recording sites in the PIT covered the region both dorsal and ventral to the PMTS. Figure 9*B* and *C* shows the RF mapping, and the results

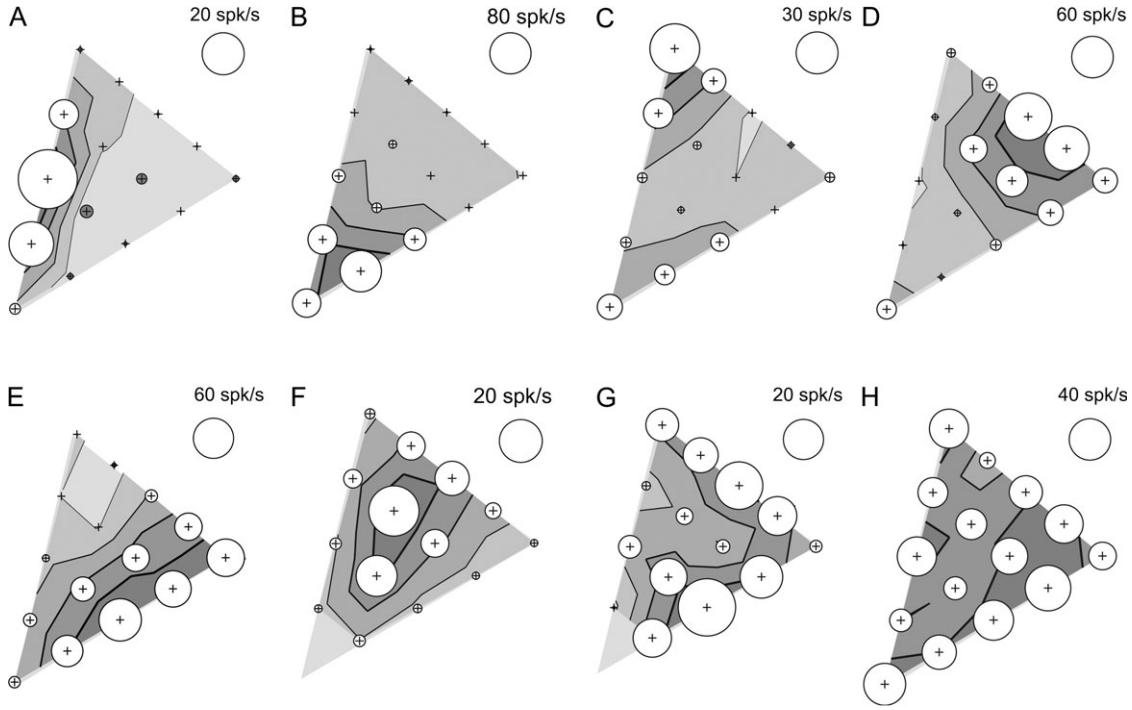

Figure 5. Color-selective responses of 8 representative PIT neurons. Responses to 14 or 15 colors with the same luminance are plotted in the same way as shown in Figure 4. Six neurons (*A–F*) recorded in the posteroventral two-thirds of the recording sites of monkey KM showed sharp color tuning. The neuron shown in G is selective for several hues (from green to yellow and from purple to blue) and that in (*H*) had very broad color tuning. These examples are arranged according to the size of the sparseness index. From (*A–H*), the sparseness index of each neuron is 0.82, 0.62, 0.48, 0.42, 0.42, 0.34, 0.25, and 0.06, respectively. A dark color set was used for the neurons in (*A–E,H*). Bright color set was used for the neurons in (*F*,G).

were strikingly similar to those obtained in monkey KM. In the PIT, most neurons in the dorsal half of the recording sites had relatively small RFs enclosing the foveal center, whereas in the ventral half, RF centers shifted out of the fovea and represented a more peripheral visual field. Furthermore, in the ventral part, we observed clear dissociation between the representation of the upper visual field in the posterior part and that of the lower visual field in the anterior part. Overall, there was a crude but clear retinotopic organization in the PIT of monkey LW, and the pattern of retinotopy is consistent with that observed in monkey KM and the TEO by Boussaoud et al. (1991). Posterior to the IOS, V4 neurons had small RFs at the fovea.

Figure 10*A* shows the distribution of the color selectivity and shape selectivity of neurons recorded in monkey LW in the same format as in Figure 3*C*. The sample of neurons examined in the PIT of LW is indicated in Table 2. Of the 220 visually responsive neurons recorded, we determined both the color and shape selectivities in 157 neurons. We found that a majority of the PIT neurons were color selective (95/157: 60.5%). Many of these neurons (64/95: 67.4%) also showed shape selectivity (red stars), whereas others (31/95: 32.6%) did not (red circles). The proportion of color-selective neurons in the PIT is lower than that observed in monkey KM. This is due to the inhomogeneous distribution of color-selective neurons in the PIT of LW. This can be seen more clearly in the distribution of the color sparseness index as shown below. On the other hand, the proportion of the shape-selective neurons among the color-selective neurons is very similar to KM, and the spatial distribution of color-selective neurons with and without shape selectivity seems to be overlapped in LW as well.

Figure 10*B* shows the distribution of the color sparseness index of LW, and the neuron with sparseness index > 0.3 is

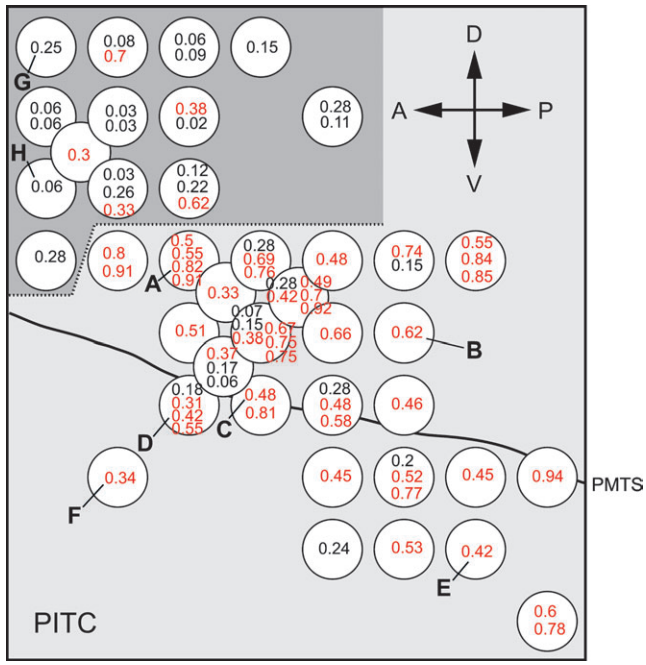

Figure 6. Distribution of the color sparseness indices over the PIT of monkey KM. The numbers are the color sparseness indices for the recorded neurons and are shown at the grid coordinates of the electrode penetration sites. Values larger than 0.3 are marked in red color. Neurons recorded from the posteroventral two-thirds of the recording sites tended to have a sharper color tuning: At recording sites ventral to the dotted line (light gray region), many neurons had a sparseness index larger than 0.3, whereas few did at the positions dorsal to the dotted line (dark gray region). We tentatively named the region ventral to the dotted line the PITC (PIT color area). Numbers marked by letters (*A–H*) indicate the neurons whose color selectivities are shown in Figure 5.

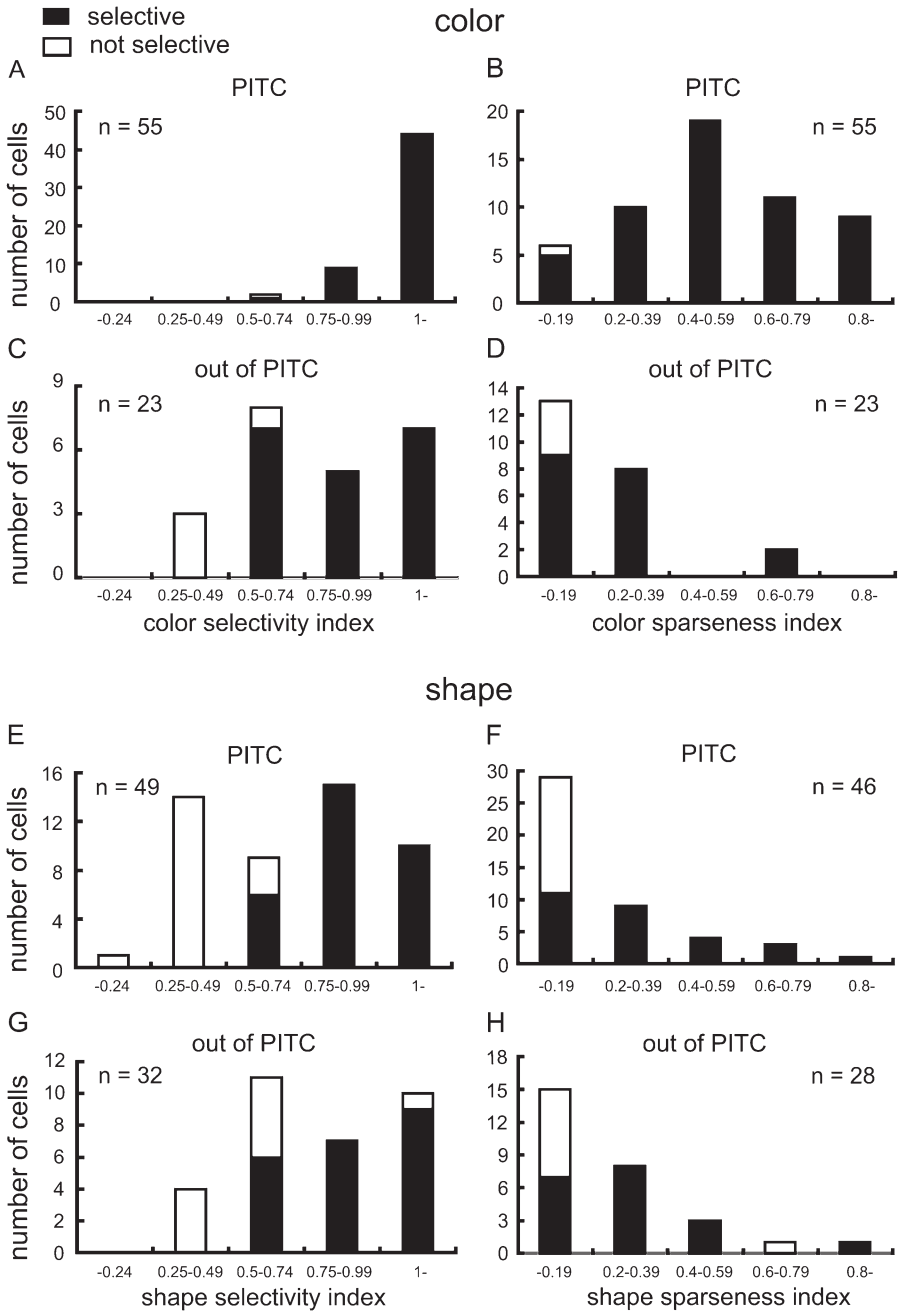

Figure 7. Selectivity and sparseness indices for neurons inside (*A*,*B*,*E*,*F*) and outside (*C*,*D*,*G*,*H*) the PITC of monkey KM. Filled bars represent neurons with stimulus selectivity and open bars those without stimulus selectivity. (*A–D*) Distributions of color selectivity (*A*,*C*) and color sparseness (*B*,*D*) indices. (*E–H*) Distributions of shape selectivity (*E*,*G*) and shape sparseness (*F*,*H*) indices. The panels in the top and third rows include cells recorded within the PITC; those in the second and fourth rows include cells recorded outside the PITC. For the test of shape selectivity, 3 neurons in the PITC and 4 neurons outside the PITC were not tested by bar stimuli (see Materials and Methods). These 7 neurons were excluded from the analysis of the shape sparseness index.

denoted by red color. Neurons with indices larger than 0.3 were mostly seen in the posteroventral two-thirds of the PIT below the dotted line (light gray region) and were very rare in the more dorsal region (dark gray region). This is consistent with the distribution of color sparseness index in KM, and we will refer to the ventral subregion as PITC. However, unlike the PITC of KM, we found that neurons with large indices are not uniformly distributed in the PITC. For example, neurons recorded from the subregion posterior to the PMTS tended to have small indices and lacked color selectivity or had only weak color selectivity although the RF sizes and positions clearly indicate this region belongs to PIT. These results may suggest that the PITC contains functionally distinct subregions with different stimulus selectivities and that such fine scale functional organization may differ across individual animals.

The results of quantitative analyses of color and shape selectivity for monkey LW are shown in Figure 11. A majority of neurons recorded both inside the PITC and outside the PITC were color selective (PITC 50/61 = 82.0%, out of PITC 6/9 = 66.7%). As expected, however, the proportion of neurons having a color sparseness index over 0.3 recorded inside the PITC (31/61 = 50.8%) was larger than that recorded outside the

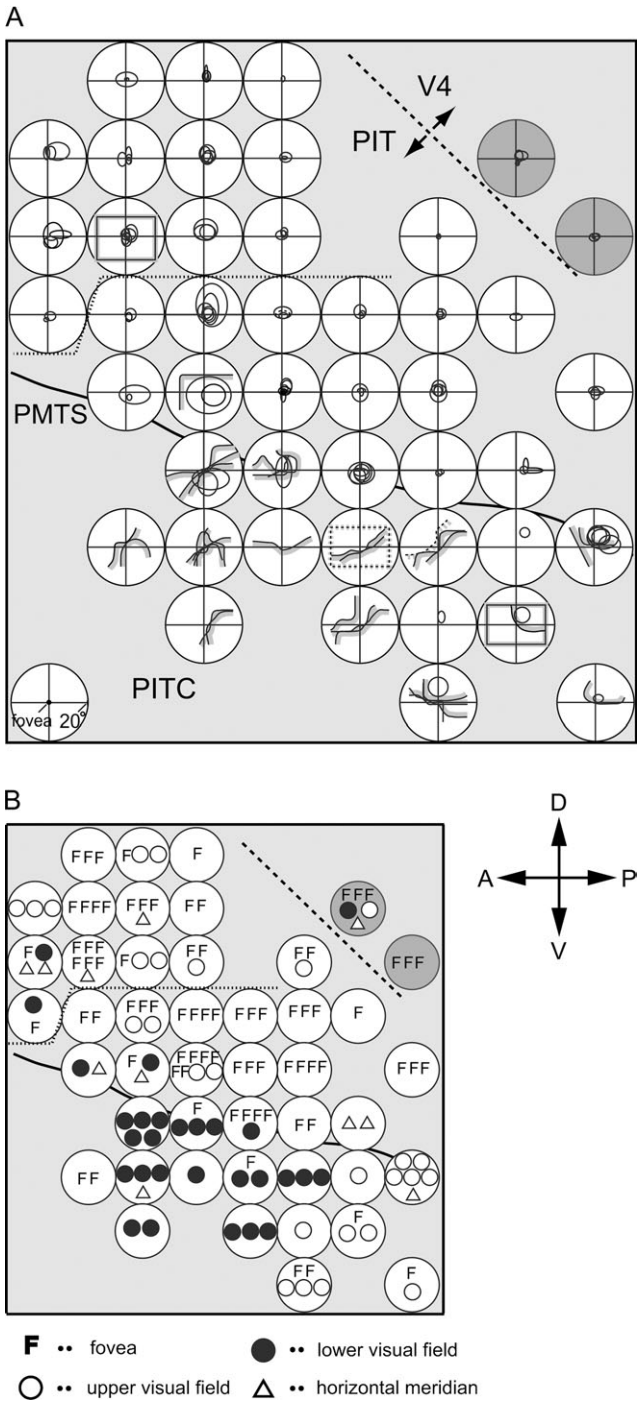

Figure 8. Distribution of RFs of PIT neurons recorded in monkey KM. (*A*) The RFs of the recorded neurons are overlaid within circles plotted at the coordinates of the electrode penetrations. White circles represent cells recorded in the PIT; 2 gray circles at the top right corner represent cells recorded outside the PIT. The center of each circle indicates the foveal center, and the edge corresponds to 20° of eccentricity. When the RF extended outside the circle, the border of the RF was shaded to indicate which part was inside of the RF. RFs shown as rectangles mean that the neurons responded at any location of the visual field examined. RFs shown by a dashed line contained the foveal center, but a stimulus presented at the foveal center did not evoke a neuronal response. In each panel, the dashed line at the top right indicates the border between area V4 and the PIT, and a dotted line indicates the border between the PITC and the rest of the PIT. (*B*) Classification of RFs into 4 categories according to the position and extent of the RFs. Symbols indicate the 4 RF categories: "F"s indicate RFs on the fovea; open and solid circles indicate RFs in the upper and lower visual fields, respectively; and triangles indicate RFs over the horizontal meridian.

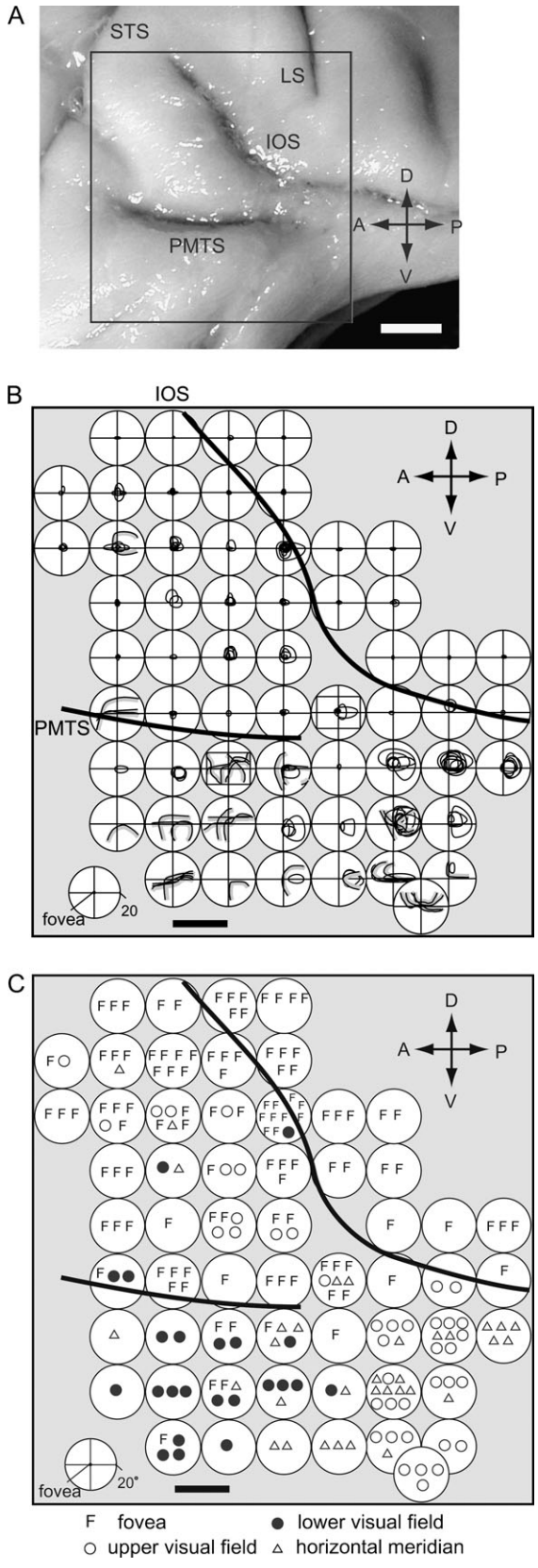

Figure 9. Recording sites in the brain of monkey LW and the distribution of RFs. (*A*) Enlarged view of the recording sites shown on the brain of monkey LW. A square indicates the area covered by the recording chamber. (*B*,*C*) Distribution of RFs recorded in monkey LW shown in the same format as in Figure 8. Scale bar, 2 mm in (*A*), 1 mm in (*B*,*C*).

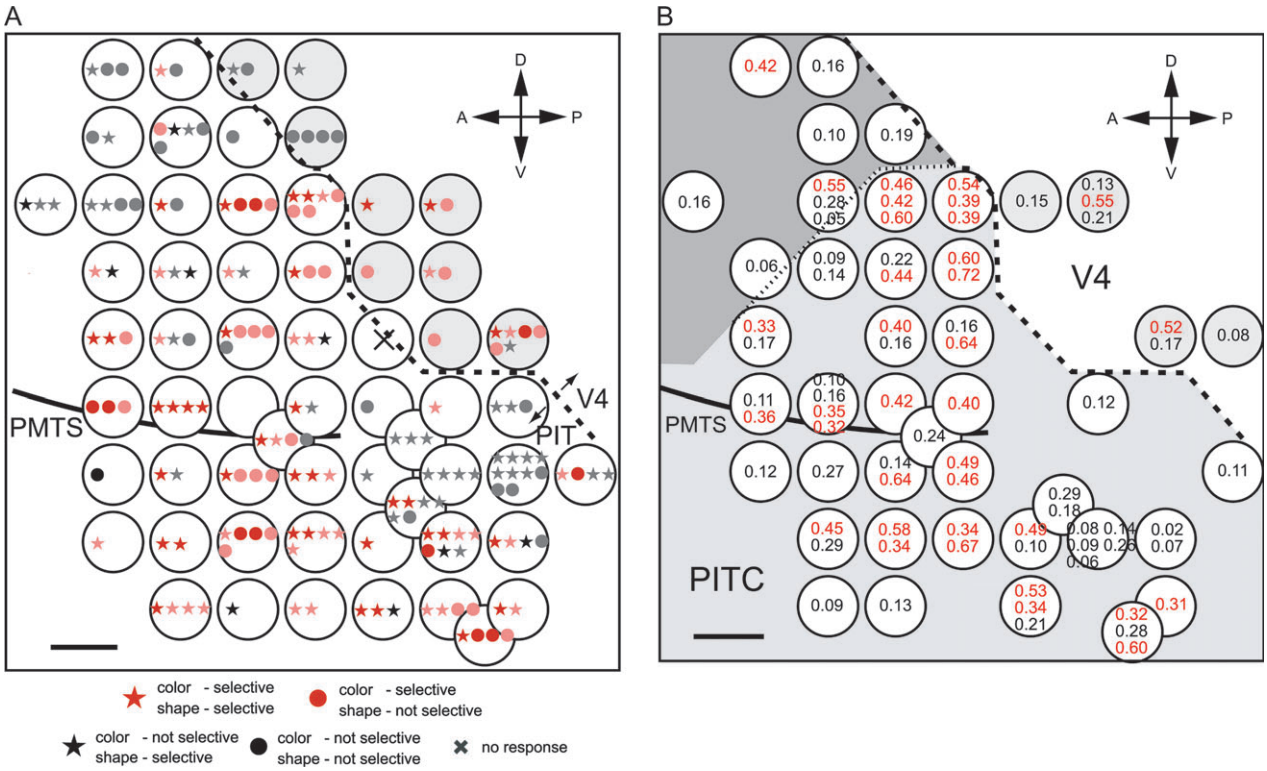

Figure 10. Distribution of color–shape selectivities in the brain of monkey LW. (*A*) Stimulus selectivity of neurons across the surface of the PIT cortex plotted in the same format as in Figure 3*C*. An open circle slightly left to the center indicates a grid hole in which visually responsive neurons were recorded but only the color selectivity was examined. (*B*) Distribution of the color sparseness indices plotted in the same format as in Figure 6. Index values > 0.3 are marked in red. The region posterior to the IOS should be area V4, and neurons recorded from this region were excluded from the sample. Broken lines in (*A*,*B*) indicate the border between PIT and V4. The presumed border of the PITC is shown by a dotted line in (*B*) Scale bar, 1 mm.

PITC (2/9 = 22.2%), although the small sample size from outside the PITC made statistical evaluation of the difference difficult. These results are generally consistent with those obtained in monkey KM. One difference is that the distribution of the color sparseness index skewed to the smaller values in monkey LW compared with that in KM (Fig. 11*B* vs. Fig. 7*B*). This seems to reflect the fact that in LW, neurons with a large color sparseness index are not uniformly distributed in the PITC as described above. The distribution of shape selectivity index and shape sparseness index was very similar to those in monkey KM, and there were no clear differences between inside and outside the PITC.

Results of Recordings from monkey MA

In monkey MA, the PMTS was situated more ventrally than in monkeys KM and LW (Fig. 2). As shown above, sharply tuned color-selective neurons were concentrated in a region across the PMTS in monkeys KM and LW, which we referred to as PITC. These results suggest that the PMTS is a good landmark for the region where sharply tuned color-selective neurons are concentrated. In order to extensively sample neurons in the cortical region around the PMTS in monkey MA as well, we attached a recording chamber at a steeper angle and in a more dorsal position, which enabled the region around the PMTS to be penetrated by the electrodes (Fig. 2*B* MA). The results obtained from this hemisphere were consistent with those from KM and LW.

The sample of neurons recorded from monkey MA is summarized in Table 3. In this hemisphere, electrodes were advanced obliquely through the cortex for a relatively long distance (Fig. 2*B* MA) and an example of electrode track is shown in Figure 12*A*. As a result, the grid coordinates do not work as a good indicator of the position of the recorded neurons with respect to the cortical surface. In this hemisphere, therefore, we constructed 2D unfolded maps of the recording sites (Fig. 12*B–D*), based on X-ray pictures of the electrode taken at the end of each recording session and MRI images of the brain, and confirmed our findings by histological examination. Using this approach, we were able to map the distributions of the neuronal selectivity (Fig. 12*B*), sparseness indices (Fig. 12*C*), and RFs (Fig. 12*D*). As expected, the recording sites included cortical regions inside of and both dorsal and ventral to the PMTS. Of the 143 visually responsive neurons recorded, we determined both the color and shape selectivities in 91 neurons. We found that most of the PIT neurons were color selective (76/91: 83.5%). Many of these neurons (57/76: 75%) also showed shape selectivity (red stars), whereas others (19/76: 25%) did not (red circles). The region around the PMTS contained many sharply tuned color-selective neurons and had a crude retinotopy. Within this region, the dorsal subregion represented the fovea, whereas the anterior part of the ventral subregion represented the lower visual field and the posterior part represented the upper visual field (Fig. 12*D*). We consider this region to correspond to the PITC identified in other monkeys (Fig. 12*C*,*D*, surrounded by a dashed line; PITC).

The results of our quantitative analysis of color selectivity in monkey MA (Fig. 13*A–D*) resembled that for other 2 monkeys, though the small sample size did not allow statistical evaluation of their similarity. Nonetheless, as expected, a larger proportion

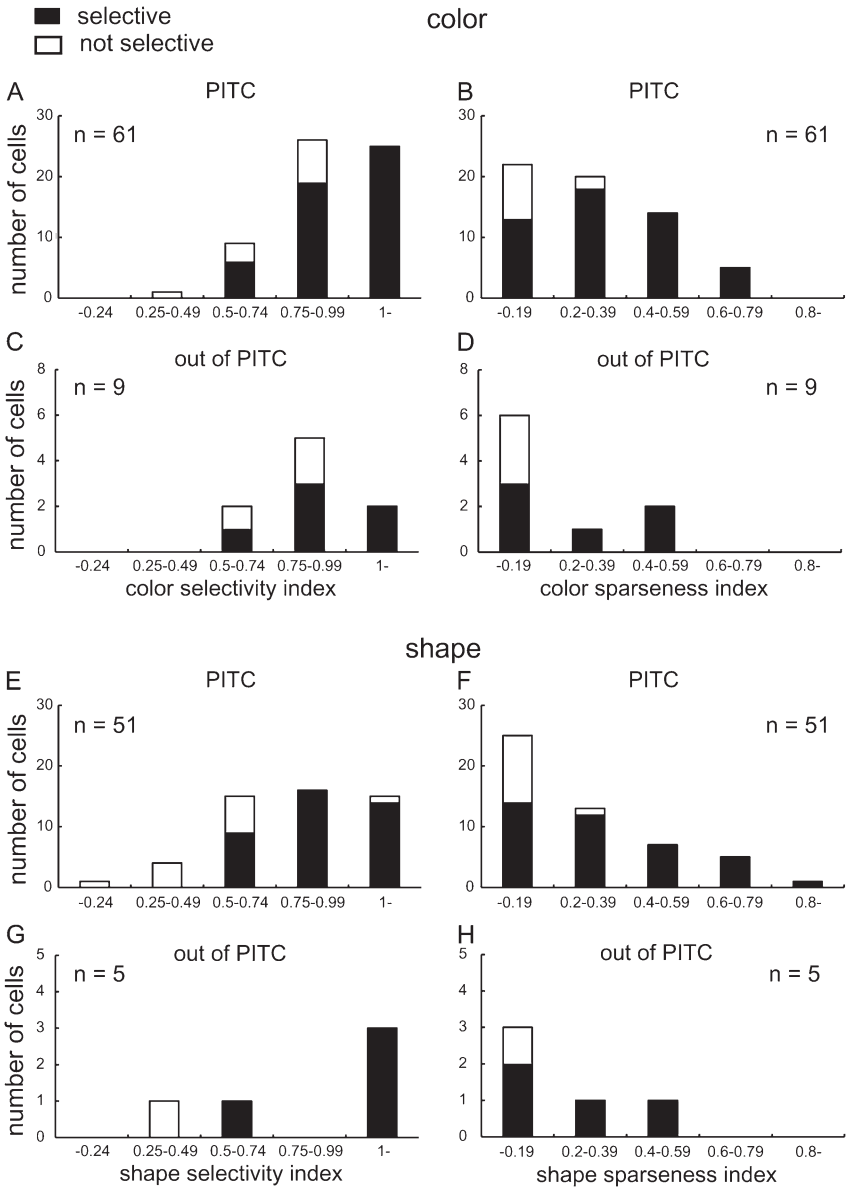

Figure 11. Distribution of selectivity and sparseness indices for neurons inside (*A*,*B*,*E*,*F*) and outside (*C*,*D*,*G*,*H*) the PITC, recorded from monkey LW. The alignment of the data is the same as in Figure 7.

of neurons (9 of 15) recorded inside the PITC had color sparseness indices larger than 0.3 than those recorded outside the PITC (only 2 of 6 neurons had values larger than 0.3). In this hemisphere, there were also differences in shape selectivity between the PITC and the region outside the PITC: Neurons inside the PITC (Fig. 13*E*) tended to show weaker shape selectivity than those outside the PITC (Fig. 13*G*).

Based on the results from 3 hemispheres of 3 monkeys, we conclude that many sharply tuned color-selective neurons exist in the region of the PIT situated around the PMTS, which we referred to as the PITC, and its position shifts depending on the location of the PMTS in individual hemispheres.

Representation of the Color Space by the Population of PITC Neurons

We found that color preference of individual PITC neurons differed from cell to cell and as a population covered the entire color space examined (Fig. 5). To more systematically determine how the population of sharply tuned color-selective neurons within the PITC represents the chromaticity diagram, we computed the average response to each color. For this purpose, we averaged the responses of PITC neurons with color sparseness indices larger than 0.3 for each color at each luminance level after the responses of each neuron were normalized to the response to the most-preferred color of the same neuron. We computed this average response to each color for the 2 monkeys (KM and LW) in which a large number of color-selective neurons were recorded. Although the responses to bright red tended to be weak in KM and those to dark red were relatively weak in LW, there was no significant variation in the average normalized responses across colors in any of the 4 distributions (Fig. 14*A*–*D*, ANOVA, $P > 0.05$). This indicates that as a whole the sharply tuned color-selective neurons in the PITC represent the entire chromaticity diagram examined.

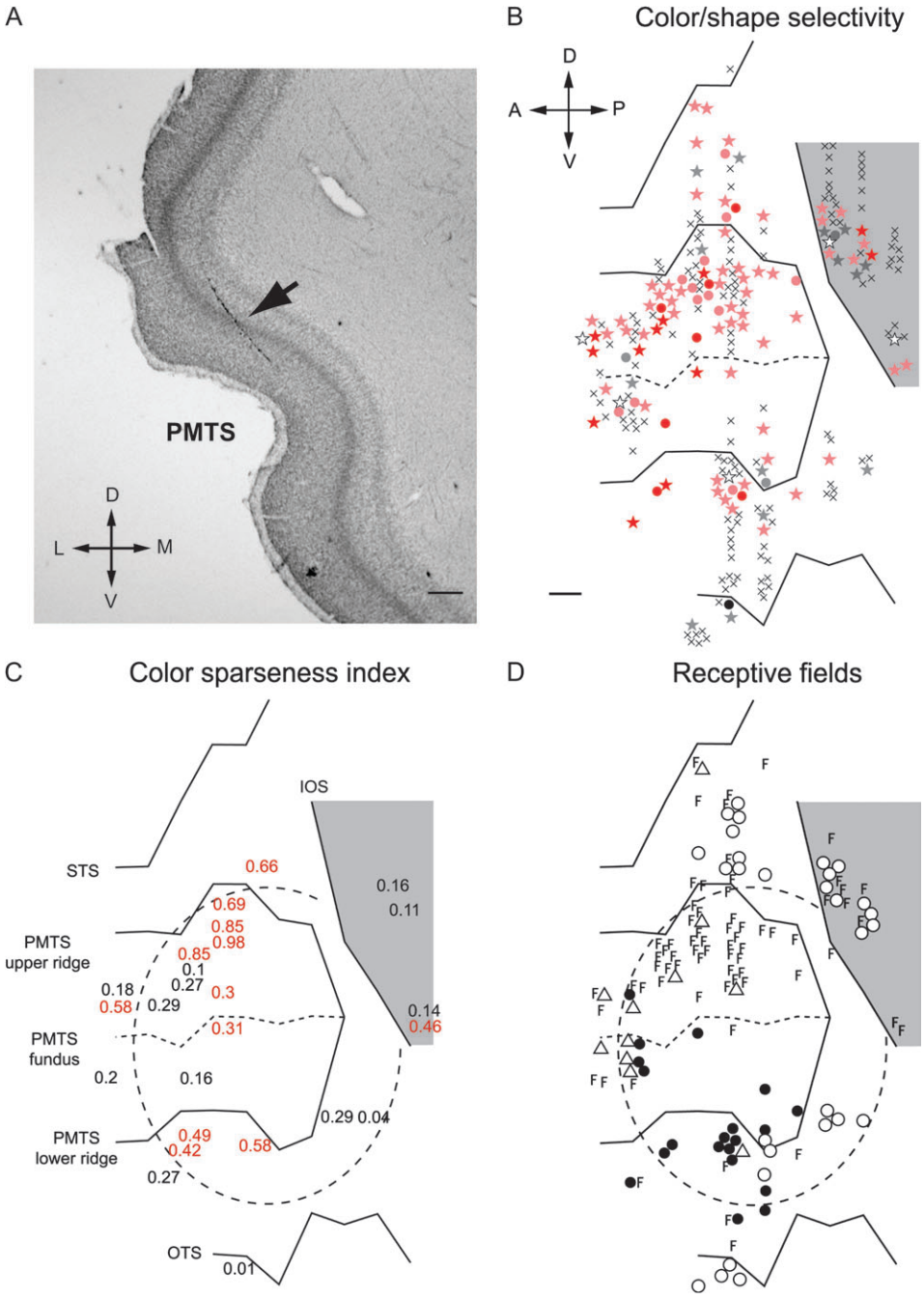

Figure 12. Distribution of the color selectivities, shape selectivities, and RFs in the PIT of monkey MA. (*A*) Cresyl violet–stained coronal section of the PIT around the PMTS. An arrow indicates the trace of an electrode penetration. In (*B–D*), the data obtained from each neuron recorded in this hemisphere are plotted at the recording sites on a 2D unfolded map. Solid lines indicate the ridges of sulci, and the broken line indicates the fundus of the PMTS. The region inside the IOS (gray region) should be area V4, and neurons recorded in this region were excluded from the sample. (*B*) Distribution of the color–shape selectivities. Crosses indicate neurons that were not driven by the visual stimuli used. Other symbols are the same as in Figure 3*C*. (*C*) Distribution of the sparseness indices; index values > 0.3 are marked in red. (*D*) Distribution of RFs classified into the same 4 categories as in Figure 9*B*. In (*B*,*C*), the presumed border of the PITC is shown as a dashed oval. Scale bar, 1 mm.

Discussion

In the present study, we systematically investigated color-selective responses within the lateral surface of the PIT cortex by recording the activities of a large number of color-selective neurons present within this area. An earlier electrophysiological study also showed the presence of color-selective neurons in this area (Tanaka et al. 1991), and imaging studies have shown that the PIT is indeed activated by color stimuli (Takechi et al. 1997; Tootell et al. 2004; Conway and Tsao 2006). To our knowledge, however, the present study is the first to systematically examine the color-selective responses of neurons in the lateral surface of PIT and to examine the distribution of the properties of neuronal color selectivity in this cortical region.

To characterize the color selectivity of each neuron, we have used color stimuli that distributed evenly on the CIE chromaticity diagram. By using this system, we can make the comparison between the neural representation of color and

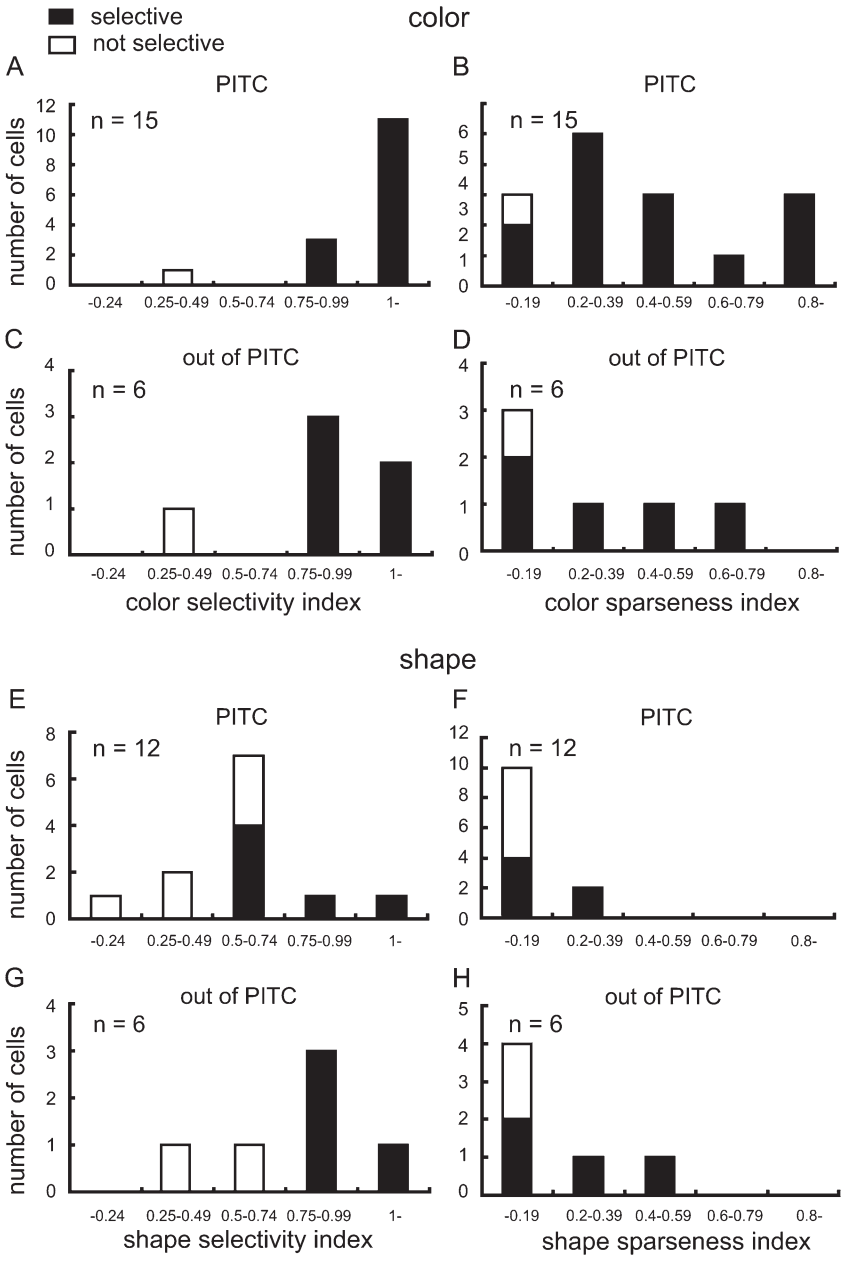

Figure 13. Distribution of selectivity and sparseness indices for neurons inside (*A*,*B*,*E*,*F*) and outside (*C*, *D*,*G*,*H*) the PITC, recorded from monkey MA. The alignment of the data is the same as in Figure 7.

various aspects of color perception of the stimulus. Each stimulus in our stimulus set had the same luminance, but it was different from the background luminance. By using such stimulus set, we were able to test the responses to all range of colors with varying hue and saturation that can be presented on our display. Although our stimulus contains both luminance and chromatic components, the luminance component was kept constant across the stimulus set, so any response difference across the stimulus set should reflect the selectivity to color. Some studies have suggested that equiluminance measurements may be different for humans and macaque monkeys (Dobkins et al. 2000), and this poses a possibility that our stimulus set contained some variation of the luminance. It is highly unlikely, however, that sharp color tuning observed in the PITC is significantly affected by such potential luminance artifact.

We found that neurons with sharp color tuning were not homogeneously distributed in the PIT; instead, they were concentrated in a particular region, which we referred to as the PITC. Neurons located outside the PITC had broader color tuning than those inside the PITC. An earlier 2-DG experiment showed that color stimuli evoke activation of patchy regions of the PIT (Tootell et al. 2004); our present findings appear consistent with that report. A more recent fMRI study using monkeys (Conway et al. 2007) has shown that color stimuli evoked activation in 5 patchy regions (called "glob"s) in V4 and 2 globs in the posterior IT cortex. One of these globs (number 5 in their paper) apparently corresponds to the PITC in the present study because it is located on the lateral surface of PIT at a location similar to the PITC. In the same study, single neuron recordings were also conducted from some of the globs

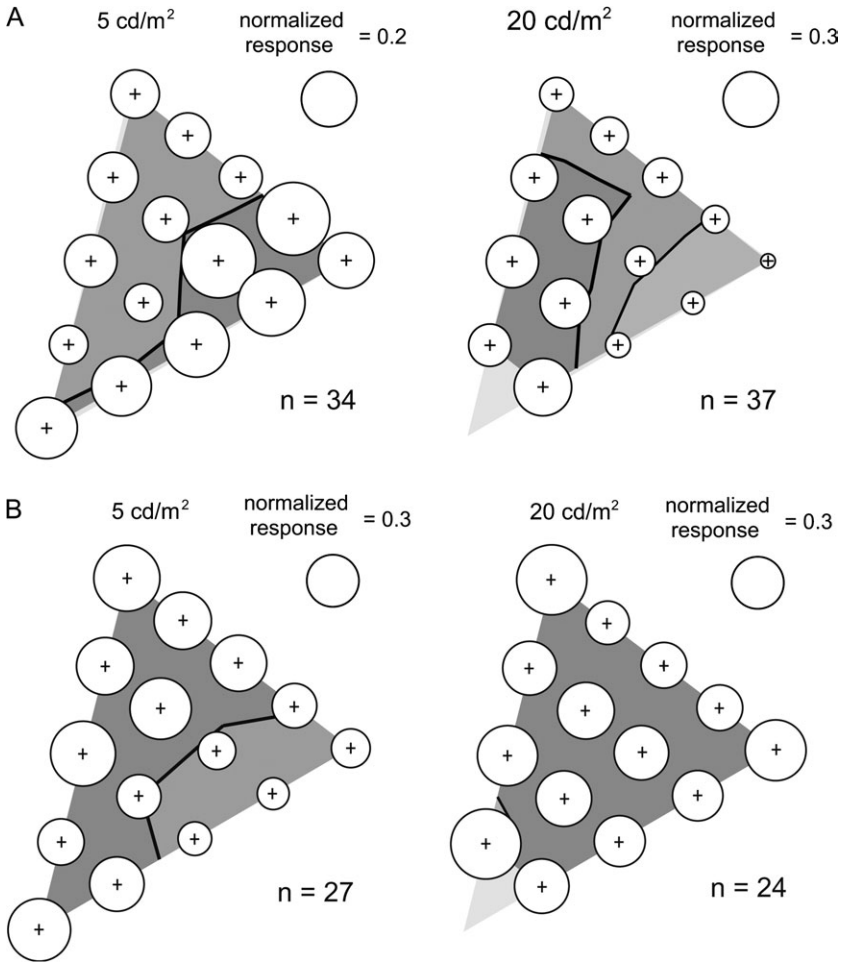

Figure 14. Average responses to each color at each luminance level of all PITC neurons with a color sparseness index of larger than 0.3. Neurons recorded from monkey KM (*A*) and LW (*B*) are shown separately. For each neuron, the response to each color was normalized by the response to the most-preferred color of the same neuron. In both (*A*,*B*), the left panel shows the responses to the dark color set (5 cd/m^2), and the right panel shows the responses to the bright color set (20 cd/m^2). As a group, PITC neurons represented the entire chromaticity diagram examined at each luminance level.

and confirmed the presence of color-selective neurons. However, they did not record neuron activities from the glob on the lateral surface of PIT that precludes direct comparison of neural properties with the present study. We do not believe that the PITC is solely devoted to color processing, as we found that numerous shape-selective neurons were also present. This is consistent with the finding of Conway et al. (2007) that neurons in the color-responsive patch in PITd in the posterior bank of STS are not only color selective but also selective for shape. In addition, we observed in 1 monkey (LW) that color-selective neurons are not uniformly distributed in the PITC. This suggests that the PITC may have functional modules with different properties of neurons. Neither do we believe that the PITC is the only region in the lateral surface of the PIT cortex involved in color processing, as we found many color-selective neurons outside the PITC. Nevertheless, sharply tuned color-selective neurons were clearly concentrated in the PITC. It has been already shown that PIT in the posterior bank of STS contains a patchy region devoted for color (Conway and Tsao 2006; Conway et al. 2007). Our present study suggests that the lateral surface of the PIT cortex also contains a subregion that plays a distinct functional role in color vision.

Functional-imaging studies in humans have shown that there exist regions selectively responsive to certain categories of visual stimuli such as faces, bodies, or scenes (Kanwisher et al. 1997; Downing et al. 2006). Likewise, recent fMRI and electrophysiological studies in monkeys revealed the presence of regions several millimeters in extent that are selectively responsive to faces (Logothetis et al. 1999; Tsao et al. 2003, 2006), body parts (Tsao et al. 2003), or color (Conway et al. 2007). The present study provides further support on the presence of such a region in the lateral surface of the posterior IT cortex with a concentration of sharply tuned color-selective neurons. It is known that the IT cortex has a columnar organization in which neurons with similar stimulus selectivities are arranged in columns perpendicular to the cortical surface and that each column forms a functional unit (Fujita et al. 1992). The dimension of each column in the IT cortex is thought to be approximately 500 μm along the cortical surface (Tanaka 1996). By contrast, the PITC identified in the present study is clearly much larger in size than the IT columns. Presumably, the PITC contains a number of columns, but how the neurons with different color selectivities are spatially arranged within the PITC still remains unclear and awaits more detailed mapping.

We mapped the RFs of PIT neurons and found there to be a crude retinotopic organization within the PITC, which was distinguished from area V4 based on its larger RF sizes and its

location anterior to the IOS. This retinotopy corresponded well to what Boussaoud et al. (1991) reported for the PIT. They reported that the retinotopic map covered its entire lateral surface ventral to the STS and named this area TEO. In our present study, we found that clear retinotopic organization was restricted to a part of the PIT that roughly corresponded to a region where sharply tuned color-selective neurons existed in relatively high density. Moreover, the position of the retinotopic map seemed to shift in coincidence with variation in the position of the PMTS. This suggests that there is a circumscribed region in and around the PMTS that has crude retinotopic organization and is involved in processing color information. As we could not identify the ventral border of the PITC, further study will be required before we know whether the overlap between the region of sharply tuned color-selective neurons and the crude retinotopic organization extends to more ventral cortical regions. Nonuniform distribution of color-selective neurons in one monkey (LW) suggests that the PITC contains functionally distinct subregions with different stimulus selectivities and that such fine scale functional organization may differ across individual animals. Another possibility would be that there exists a separate region between PITC and V4. In monkey LW, color selectivity tended to be weak and broad in the most posterior part of the PITC where neurons had RFs on the horizontal meridian and in the upper visual field. This may be explained by the presence of a separate region. A possible existence of a region of a narrow strip between V4 and TEO that represents the upper visual field has been argued (Van Essen et al. 1990; Boussaoud et al. 1991). Further study should be necessary to elucidate the functional organization within the PITC and the surrounding region.

The PIT receives major visual input from area V4 and weaker but significant projections from areas V2 and V3 (Distler et al. 1993). All of these areas contain color-selective neurons and are candidate sources for the color signals to the PIT. V2 neurons projecting to the PIT are localized within cytochrome oxidase (CO)–poor interstripe regions and CO-rich thin stripes (Nakamura et al. 1993), where color-sensitive neurons are concentrated (DeYoe and Van Essen 1985; Hubel and Livingstone 1987). The PIT, in turn, sends outputs to area TE, where there are many color-selective neurons (Komatsu et al. 1992). An anatomical study showed that neurons in the region near the PMTS densely project to an area slightly lateral to the anterior middle temporal sulcus (AMTS) within area TE (Saleem et al. 1993) where color-selective neurons are concentrated (Yasuda et al. 2004). Taken together, these findings suggest that the PITC may be an important site through which color signals are relayed from early visual areas to more anterior regions in area TE.

We also assessed the shape selectivity of the neurons studied and found that many were selective for both color and shape and that shape-selective neurons were distributed across the entire area of the PIT studied. This result is consistent with earlier findings that shape-selective neurons are present within the PIT (Tanaka et al. 1991; Kobatake and Tanaka 1994; Brincat and Connor 2004) and that the ablation of this area causes a severe deficit in shape discrimination (Iwai and Mishkin 1969). Within the PITC, we also found that color-selective neurons with and without shape selectivity were intermingled, which suggests that the processing of color and shape information are closely related in the PIT. PIT may be an important stage at which color information is added to shape information to construct an object image.

Earlier studies have shown that lesions within the PIT affect monkeys' ability of shape discrimination (Iwai and Mishkin 1969) and visual attention (De Weerd et al. 1999); however, selective lesion of the PIT has failed to cause a clear deficit in color discrimination (Huxlin et al. 2000). On the other hand, a number of studies have shown that lesions affecting the entire IT cortex or area TE do cause deficits in color discrimination (Horel 1994; Heywood et al. 1995; Buckley et al. 1997; Huxlin et al. 2000; Cowey et al. 2001). These results suggest that the TE plays an essential role in color discrimination and that color information can be conveyed to area TE, even when the PIT is damaged. V4 neurons are known to project to the posterior part of the TE (Van Essen et al. 1990). This projection could play a crucial role when a monkey with damage in the PIT performs color discrimination. On the other hand, lesions restricted in V4 does not cause clear deficit in color discrimination (Heywood et al. 1992). In this condition, direct projections from areas V2 and V3 to the PIT cortex bypassing V4 (Nakamura et al. 1993) should play a crucial role. Presumably, the neural pathway carrying the color information to TE consists of multiple pathways, and the PITC plays an important role as a relay station in one of these pathways. We may conceive that area V4 and the PITC play complemental roles in such multiple pathways for color vision.

Funding

Ministry of Education, Culture, Sports, Science and Technology of Japan (Japanese Grant-in-Aid for Scientific Research (B)[16300103] and a grant for Scientific Research on Priority Areas "System study on higher-order brain functions" [17022040]).

Notes

We thank M. Togawa for technical assistance and K. Koida for help with the data analysis. *Conflict of Interest:* None declared.

Address correspondence to Hidehiko Komatsu, PhD, Division of Sensory and Cognitive Information, National Institute for Physiological Sciences, Myodaiji, Okazaki 444-8585, Japan. Email: komatsu@nips.ac.jp.

References

Bonin GV, Bailey P. 1947. The neocortex of *Macaca mulatta*. Urbana (IL): University of Illinois Press.

Boussaoud D, Desimone R, Ungerleider LG. 1991. Visual topography of area TEO in the macaque. J Comp Neurol. 306:554–575.

Brincat SL, Connor CE. 2004. Underlying principles of visual shape selectivity in posterior inferotemporal cortex. Nat Neurosci. 7:880–886.

Buckley MJ, Gaffan D, Murray EA. 1997. Functional double dissociation between two inferior temporal cortical areas: perirhinal cortex versus middle temporal gyrus. J Neurophysiol. 77:587–598.

Conway BR, Moeller S, Tsao DY. 2007. Specialized color modules in macaque extrastriate cortex. Neuron. 56:560–573.

Conway BR, Tsao DY. 2006. Color architecture in alert macaque cortex revealed by fMRI. Cereb Cortex. 16:1604–1613.

Cowey A, Heywood CA, Irving-Bell L. 2001. The regional cortical basis of achromatopsia: a study on macaque monkeys and an achromatopsic patient. Eur J Neurosci. 14:1555–1566.

Crist CF, Yamasaki DS, Komatsu H, Wurtz RH. 1988. A grid system and a microsyringe for single cell recording. J Neurosci Methods. 26:117–122.

De Weerd P, Peralta MR, 3rd, Desimone R, Ungerleider LG. 1999. Loss of attentional stimulus selection after extrastriate cortical lesions in macaques. Nat Neurosci. 2:753–758.

DeYoe EA, Van Essen DC. 1985. Segregation of efferent connections and receptive field properties in visual area V2 of the macaque. Nature. 317:58–61.
Distler C, Boussaoud D, Desimone R, Ungerleider LG. 1993. Cortical connections of inferior temporal area TEO in macaque monkeys. J Comp Neurol. 334:125–150.
Dobkins KR, Thiele A, Albright TD. 2000. Comparison of red-green equiluminance points in humans and macaques: evidence for different L:M cone ratios between species. J Opt Soc Am A. 17:545–556.
Downing PE, Chan AW, Peelen MV, Dodds CM, Kanwisher N. 2006. Domain specificity in visual cortex. Cereb Cortex. 16:1453–1461.
Fujita I, Tanaka K, Ito M, Cheng K. 1992. Columns for visual features of objects in monkey inferotemporal cortex. Nature. 360:343–346.
Heywood CA, Gadotti A, Cowey A. 1992. Cortical area V4 and its role in the perception of color. J Neurosci. 12:4056–4065.
Heywood CA, Gaffan D, Cowey A. 1995. Cerebral achromatopsia in monkeys. Eur J Neurosci. 7:1064–1073.
Hikosaka K. 1998. Representation of foveal visual fields in the ventral bank of the superior temporal sulcus in the posterior inferotemporal cortex of the macaque monkey. Behav Brain Res. 96:101–113.
Horel JA. 1994. Retrieval of color and form during suppression of temporal cortex with cold. Behav Brain Res. 65:165–172.
Hubel DH, Livingstone MS. 1987. Segregation of form, color, and stereopsis in primate area 18. J Neurosci. 7:3378–3415.
Huxlin KR, Saunders RC, Marchionini D, Pham HA, Merigan WH. 2000. Perceptual deficits after lesions of inferotemporal cortex in macaques. Cereb Cortex. 10:671–683.
Iwai E, Mishkin M. 1969. Further evidence on the locus of the visual area in the temporal lobe of the monkey. Exp Neurol. 25:585–594.
Kanwisher N, McDermott J, Chun MM. 1997. The fusiform face area: a module in human extrastriate cortex specialized for face perception. J Neurosci. 17:4302–4311.
Kobatake E, Tanaka K. 1994. Neuronal selectivities to complex object features in the ventral visual pathway of the macaque cerebral cortex. J Neurophysiol. 71:856–867.
Koida K, Komatsu H. 2007. Effects of task demands on the responses of color-selective neurons in the inferior temporal cortex. Nat Neurosci. 10:108–116.
Komatsu H, Ideura Y. 1993. Relationships between color, shape, and pattern selectivities of neurons in the inferior temporal cortex of the monkey. J Neurophysiol. 70:677–694.
Komatsu H, Ideura Y, Kaji S, Yamane S. 1992. Color selectivity of neurons in the inferior temporal cortex of the awake macaque monkey. J Neurosci. 12:408–424.
Logothetis NK, Guggenberger H, Peled S, Pauls J. 1999. Functional imaging of the monkey brain. Nat Neurosci. 2:555–562.
Matsumora T, Koida K, Komatsu H. 2008. Relationship between color discrimination and neural responses in the inferior temporal cortex of the monkey. J Neurophysiol. 100:3361–3374.
Nakamura H, Gattass R, Desimone R, Ungerleider LG. 1993. The modular organization of projections from areas V1 and V2 to areas V4 and TEO in macaques. J Neurosci. 13:3681–3691.
Robinson DA. 1963. A method of measuring eye movement using a scleral search coil in a magnetic field. IEEE Trans Biomed Eng. 10:137–145.
Rolls ET, Tovee MJ. 1995. Sparseness of the neuronal representation of stimuli in the primate temporal visual cortex. J Neurophysiol. 73: 713–726.
Saleem KS, Tanaka K, Rockland KS. 1993. Specific and columnar projection from area TEO to TE in the macaque inferotemporal cortex. Cereb Cortex. 3:454–464.
Schein SJ, Desimone R. 1990. Spectral properties of V4 neurons in the macaque. J Neurosci. 10:3369–3389.
Takechi H, Onoe H, Shizuno H, Yoshikawa E, Sadato N, Tsukada H, Watanabe Y. 1997. Mapping of cortical areas involved in color vision in non-human primates. Neurosci Lett. 230:17–20.
Tanaka K. 1996. Inferotemporal cortex and object vision. Annu Rev Neurosci. 19:109–139.
Tanaka K, Saito H, Fukada Y, Moriya M. 1991. Coding visual images of objects in the inferotemporal cortex of the macaque monkey. J Neurophysiol. 66:170–189.
Tootell RB, Nelissen K, Vanduffel W, Orban GA. 2004. Search for color 'center(s)' in macaque visual cortex. Cereb Cortex. 14:353–363.
Tsao DY, Freiwald WA, Knutsen TA, Mandeville JB, Tootell RB, Boussaoud D, Desimone R, Ungerleider LG. 2003. Faces and objects in macaque cerebral cortex. Nat Neurosci. 6:989–995.
Tsao DY, Freiwald WA, Tootell RB, Livingstone MS. 2006. A cortical region consisting entirely of face-selective cells. Science. 311:670–674.
Van Essen DC, Felleman DJ, DeYoe EA, Olavarria J, Knierim J. 1990. Modular and hierarchical organization of extrastriate visual cortex in the macaque monkey. Cold Spring Harb Symp Quant Biol. 55:679–696.
Van Essen DC, Maunsell JH. 1980. Two-dimensional maps of the cerebral cortex. J Comp Neurol. 191:255–281.
Vinje WE, Gallant JL. 2000. Sparse coding and decorrelation in primary visual cortex during natural vision. Science. 287:1273–1276.
Yasuda M, Koida K, Goda N, Komatsu H. 2004. Regional specialization for color processing in area TE of the monkey. Soc Neurosci Abst. 34:174.1.
Zeki SM. 1973. Colour coding in rhesus monkey prestriate cortex. Brain Res. 53:422–427.